Acta Cryst. (1996). **B52**, 651–661

Structural Studies on Monofluorinated Derivatives of the Phytohormone Indole-3-acetic Acid (Auxin)†

SNJEŽANA ANTOLIĆ,[a] BISERKA KOJIĆ-PRODIĆ,[a]* SANJA TOMIĆ,[a] BILJANA NIGOVIĆ,[a] VOLKER MAGNUS[a] AND JERRY D. COHEN[b]

[a]*Rudjer Bošković Institute, POB 1016, 10000 Zagreb, Croatia, and* [b]*Horticultural Crops Quality Laboratory Beltsville, Agricultural Research Center, Agricultural Research Service, USDA, Beltsville, MD 20705-2350, USA. E-mail: kojic@olimp.irb.hr*

(*Received 18 October 1995; accepted 1 December 1995*)

Abstract

As part of the molecular recognition studies on the phytohormone indole-3-acetic acid (IAA) a series of fluorinated IAA's has been examined. The phenyl ring substitution at positions 4, 5, 6 and 7 resulted in four compounds, which were analyzed. Structure–activity correlation includes the analysis of their molecular conformations, based on the X-ray diffraction and computational chemistry results, and bioactivity determinations in the *Avena* coleoptile and the *Pisum sativum* stem straight-growth tests, lipophilicity and UV absorbance. The conformations of monofluorinated IAA's and a free hormone are defined by rotations about two bonds: one describes the relative orientation of a side chain towards the indole plane and the second the orientation of the carboxylic group. The results of X-ray structure analysis revealed the folded shape of the molecules in all compounds studied. Molecular mechanics and dynamics located the folded conformation as the local minimum, but failed to detect the planar conformation as one of the local minima, which according to *ab initio* results on IAA and 4-Cl-IAA could also be possible. Crystal data at 295 K for 4-F-IAA and at 297 K for 5-F-IAA, and at 100 K for 6-F-IAA and 7-F-IAA using Mo $K\alpha$ radiation (λ = 0.71073 Å) and Cu $K\alpha$ (λ = 1.5418 Å, for 7-F-IAA), are as follows: 4-F-IAA, $C_{10}H_8NO_2F$, M_r = 193.18, monoclinic, $C2/c$, a = 17.294 (5), b = 13.875 (4), c = 7.442 (4) Å, β = 103.88 (6)°, V = 1734 (1) Å^3, Z = 8, D_x = 1.480 g cm^{-3}, μ = 1.1 cm^{-1}, $F(000)$ = 800, R = 0.043, wR = 0.044 for 823 symmetry-independent [$I \geq 3\sigma(I)$] reflections; 5-F-IAA, $C_{10}H_8NO_2F$, monoclinic, $P2_1/c$, a = 19.284 (5), b = 5.083 (4), c = 9.939 (4) Å, β = 117.28 (6)°, V = 865.9 (1) Å^3, Z = 4, D_x = 1.482 g cm^{-3}, μ = 1.1 cm^{-1}, $F(000)$ = 400, R = 0.062, wR = 0.057 for 729 symmetry-independent [$I \geq 3\sigma(I)$] reflections; 6-F-IAA, $C_{10}H_8NO_2F$, monoclinic, $P2_1/a$, a = 9.360 (1), b = 5.167 (4), c = 17.751 (4) Å, β = 93.75 (1)°, V = 856.7 (8) Å^3, Z = 4, D_x = 1.498 g cm^{-3}, μ = 1.1 cm^{-1}, $F(000)$ = 400, R = 0.048, wR = 0.048 for 1032 symmetry-independent [$I \geq 2\sigma(I)$] reflections; 7-F-IAA, $C_{10}H_8NO_2F$, monoclinic, $P2_1/a$, a = 9.935 (5), b = 5.0059 (4), c = 17.610 (1) Å, β = 102.13 (1)°, V = 856.3 (1) Å^3, Z = 4, D_x = 1.498 g cm^{-3}, μ = 9.8 cm^{-1} (Cu $K\alpha$), $F(000)$ = 400, R = 0.035, wR = 0.040 for 1504 symmetry-independent [$I \geq 2\sigma(I)$] reflections.

1. Introduction

The structural parameters governing the plant growth-promoting properties of the natural auxin indole-3-acetic acid (IAA) and of a host of, mostly synthetic, functional analogs have been the subject of much controversy. To provide firm foundations for such discussions, X-ray crystallography supplemented by molecular mechanics and dynamics calculations was used to determine the molecular structures of 5-*n*-alkylated and ring-chlorinated indole-3-acetic acids in the solid state and in aqueous solution (Kojić-Prodić, Nigović, Tomić *et al.*, 1991; Nigović *et al.*, 1996). This approach is extended herein to their ring-fluorinated analogs. Substitution of hydrogen by fluorine is used in medicinal chemistry to manipulate the metabolic stability of, and the electron distribution in, pharmacologically active molecules without inflicting major changes on other physicochemical properties (Filler, 1993). Indeed, the van der Waals radius of the fluorine introduced only slightly exceeds that of hydrogen [1.2 for H and 1.35 Å for F (Bondi, 1964)] and the increment in lipophilicity is among the smallest known (Fujita, Iwasa & Hansch, 1964). However, electron affinity is significantly different (0.8 eV for H and 3.5 eV for F in the gas phase at 0 K). Fluorinated plant growth regulators are receiving increased attention. A novel fluorinated plant growth regulator, (*S*)-(+)-4,4,4-trifluoro-3-(indole-3-)butyric acid, was synthesized and its inhibitory effect on *Avena* coleoptile elongation was discovered (Katayama, Kato, Kimoto & Fuji, 1995). As far as the natural auxin indole-3-acetic acid (IAA) is

---

† The authors dedicate this paper to the 65th anniversary of Professor Dr Dieter Klämbt, Rheinische Friedrich–Wilhelms Universität, Bonn, who has contributed much to the molecular biology of the auxins.

concerned, its 5-fluoro derivative (5-F-IAA) showed activity in a variety of bioassays (Hoffmann, Fox & Bullock, 1952; Porter & Thimann, 1965; Böttger, Engvild & Soll, 1978; Engvild, 1978; Katekar & Geissler, 1983; Zažimalova & Kutaček, 1985) and an affinity towards a crude auxin-binding protein from wheat shoots (Zažimalova & Kutaček, 1985). Indole-3-acetic acids fluorinated at any of the four possible positions in the phenyl moiety (Scheme I) have so far only been tested for their ability to sustain the growth of deseeded pea pods (Reinecke, Ozga & Magnus, 1995). Here we demonstrate that the same compounds are at least as stimulatory as IAA in stem (coleoptile) elongation assays. 4-F-IAA is an extremely potent auxin in the *Avena* coleoptile straight-growth test. According to the same type of tests performed on a *Zea mays* mutant, 4-F-IAA is more active than IAA (Klämbt, private communication).

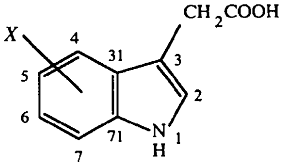

4-F-IAA, 5-F-IAA, 6-F-IAA, 7-F-IAA; *X* = F

Scheme I. Structural formulae of monofluorinated indole-3-acetic acids and their abbreviations used.

The auxin activity of the fluorinated IAA's is discussed in terms of molecular structure and physicochemical constants, such as lipophilicity.

2. Experimental

2.1. *X-ray measurements and structure determination*

5-Fluoroindole-3-acetic acid was obtained from Sigma, while 4-fluoroindole-3-acetic acid (Somei, Kizu, Kunimoto & Yamada, 1985) and 6-fluoroindole-3-acetic acid (Bergmann & Pelchowicz, 1959) were obtained from commercial fluoroindoles, *via* the corresponding fluorogramines. 7-Fluoroindole-3-acetic acid was prepared by Fischer cyclization of 4-(2-fluorophenylhydrazono)butyric acid (Reinecke, Ozga & Magnus, 1995). The crystals suitable for X-ray structure analysis were prepared by slow evaporation of 2 ml solutions containing 10–15 mg ml^{-1} of compounds in the solvent mixtures methanol + propan-2-ol + water (1:1:1, volume) for 4-F-IAA and 5-F-IAA, methanol + water (1:1, volume) for 6-F-IAA and 7-F-IAA. The crystals were grown at room temperature over 3 d and for 5-F-IAA over 2 weeks.

The compounds studied are achiral and crystallize in the centrosymmetric space groups: $P2_1/c$ ($P2_1/a$) and $C2/c$ (a single case). Data were collected on an Enraf–Nonius CAD-4 diffractometer (Table 1) in the dark (due to the sensitivity to light) with graphite-monochromated Mo $K\alpha$ and Cu $K\alpha$ (for 7-F-IAA) radiation and rescaled for decay on the basis of intensity reduction of two standard reflections measured every 100 reflections. The maximum reduction was 1.5% for 5-F-IAA. Lorentz and polarization corrections were applied using the Enraf–Nonius *SDP/VAX* package (B. A. Frenz & Associates Inc., 1982). Structures were solved by direct methods using the program *SHELX*86 (Sheldrick,1985) and refined by *SHELX*76 (Sheldrick, 1976) with a full-matrix least-squares procedure minimizing $\Sigma w(|F_o| - |F_c|)^2$ on F values. Difference-Fourier maps were used to locate the H atoms. The non-H atoms were refined anisotropically. The H-atom coordinates and isotropic displacement parameters were refined. Details of the refinement procedures are listed in Table 1. Scattering factors are those included in *SHELX*76 (Sheldrick, 1976). Molecular geometry was calculated by the program package *EUCLID* (Spek, 1982). Drawings were prepared by the *PLUTON* program incorporated into *EUCLID* and *ORTEP*II (Johnson, 1976). The final atomic coordinates and equivalent isotropic thermal parameters are listed in Table 2.† Calculations were performed on MicroVAXII and INDIGO-2 computers of the X-ray Laboratory, Rudjer Bošković Institute, Zagreb, Croatia.

2.2. *Physicochemical measurements*

UV spectra (in 95% ethanol) were measured on a Beckman DU-50 single-beam spectrophotometer (Table 3). Relative lipophilicities were calculated from retention times on a reversed-phase HPLC column (250 × 4 mm i.d.) packed with Spherisorb C18-ODS2 (Chrom Tech, Apple Valley, Minnesota, USA), particle size 5 μm, and eluted at 303 K with 25% (*v*/*v*) aqueous acetonitrile containing 0.1 *N* acetic acid. The effluent was monitored for absorbance at 280 nm. The void volume was determined from the retention time (t_0) of potassium oxalate. The ‘capacity factors’ (k') for IAA and its ring-substituted derivatives were calculated as $(t_i - t_0)/t_0$, wherein t_i is the retention time of the respective indolic compound (Krstulović & Brown, 1982). The increment in lipophilicity caused by substitution (Leo, Hansch & Elkins, 1971) was then computed as $\Pi = \log P_{\text{substituted IAA}} - \log P_{\text{IAA}} = \log k'_{\text{substituted IAA}} - \log k'_{\text{IAA}}$ (Table 4, because the partition coefficient P equals k' multiplied by a factor which is the same for all compounds chromatographed on the same column). For the UV spectra and lipophilicity measurements the fluorinated and chlorinated IAA's were included in order to see the effect of electronegativity.

---

† Lists of atomic coordinates, anisotropic displacement parameters and structure factors have been deposited with the IUCr (Reference: SE0185). Copies may be obtained through The Managing Editor, International Union of Crystallography, 5 Abbey Square, Chester CH1 2HU, England.

Table 1. *Experimental details*

	4-F-IAA	5-F-IAA	6-F-IAA	7-F-IAA
Crystal data				
Chemical formula	$C_{10}H_8FNO_2$	$C_{10}H_8FNO_2$	$C_{10}H_8FNO_2$	$C_{10}H_8FNO_2$
Chemical formula weight	193.18	193.18	193.18	193.18
Cell setting	Monoclinic	Monoclinic	Monoclinic	Monoclinic
Space group	$C2/c$	$P2_1/c$	$P2_1/a$	$P2_1/a$
a (Å)	17.294 (5)	19.284 (5)	9.360 (1)	9.935 (5)
b (Å)	13.875 (4)	5.083 (4)	5.167 (4)	5.0059 (4)
c (Å)	7.442 (4)	9.939 (4)	17.751 (4)	17.610 (1)
β (°)	103.88 (6)	117.28 (6)	93.75 (1)	102.13 (1)
V (Å^3)	1734 (1)	865.9 (1)	856.7 (8)	856.3 (1)
Z	8	4	4	4
D_x (Mg m^{-3})	1.480	1.482	1.498	1.498
Radiation type	Mo $K\alpha$	Mo $K\alpha$	Mo $K\alpha$	Cu $K\alpha$
Wavelength (Å)	0.71073	0.71073	0.71073	1.5418
No. of reflections for cell parameters	25	25	15	25
θ range (°)	6–15	6–17	18–25	25–46
μ (mm^{-1})	0.11	0.11	0.11	0.98
Temperature (K)	295	297	100	100
Crystal form	Prismatic	Prismatic	Prismatic	Plate
Crystal size (mm)	0.45 × 0.17 × 0.14	0.60 × 0.45 × 0.15	0.36 × 0.27 × 0.10	0.28 × 0.28 × 0.08
Crystal color	Colorless	Colorless	Colorless	Colorless
Data collection				
Diffractometer	Enraf–Nonius CAD-4	Enraf–Nonius CAD-4	Enraf–Nonius CAD-4	Enraf–Nonius CAD-4
Data collection method	ω–θ	ω–2θ	ω–2θ	ω–2θ
Absorption correction	None	None	None	None
No. of measured reflections	2566	1806	2082	2070
No. of independent reflections	1293	1302	1379	1635
No. of observed reflections	823	729	1032	1504
Criterion for observed reflections	$I > 3\sigma(I)$	$I > 3\sigma(I)$	$I > 2\sigma(I)$	$I > 2\sigma(I)$
R_{int}	0.0342	0.0596	0.0371	0.019
θ_{max} (°)	25	25	26.32	74.33
Range of h, k, l	$0 \rightarrow h \rightarrow 20$ $0 \rightarrow k \rightarrow 16$ $-8 \rightarrow l \rightarrow 8$	$0 \rightarrow h \rightarrow 11$ $0 \rightarrow k \rightarrow 6$ $-20 \rightarrow l \rightarrow 20$	$0 \rightarrow h \rightarrow 11$ $-6 \rightarrow k \rightarrow 0$ $-22 \rightarrow l \rightarrow 22$	$-12 \rightarrow h \rightarrow 0$ $0 \rightarrow k \rightarrow 6$ $-22 \rightarrow l \rightarrow 22$
No. of standard reflections	2	2	2	2
Frequency of standard reflections	Every 100 reflections	Every 100 reflections	Every 100 reflections	Every 100 reflections
Intensity decay (%)	<1	1.5	<1	<1
Refinement				
Refinement on	F	F	F	F
R	0.043	0.062	0.048	0.035
wR	0.044	0.057	0.048	0.04
S	1.13	0.91	0.80	0.39
No. of reflections used in refinement	823	729	1032	1504
No. of parameters used	159	159	159	159
H-atom treatment	All H-atom parameters refined	All H-atom parameters refined	All H-atom parameters refined	All H-atom parameters refined
Weighting scheme	$w = k/[\sigma^2(F_o) + gF_o^2]$, where $g = 0.000528$	$w = k/[\sigma^2(F_o) + gF_o^2]$, where $g = 0.000100$	$w = k/[\sigma^2(F_o) + gF_o^2]$, where $g = 0.001346$	$w = k/[\sigma^2(F_o) + gF_o^2]$, where $g = 0.000338$
$(\Delta/\sigma)_{\text{max}}$	−0.007	0.092	0.001	0.080
$\Delta\rho_{\text{max}}$ (e Å^{-3})	0.17	0.19	0.23	0.22
$\Delta\rho_{\text{min}}$ (e Å^{-3})	−0.24	−0.28	−0.30	−0.18
Extinction method	None	None	None	None
Source of atomic scattering factors	*SHELX*76 (Sheldrick, 1976)	*SHELX*76 (Sheldrick, 1976)	*SHELX*76 (Sheldrick, 1976)	*SHELX*76 (Sheldrick, 1976)

2.3. *Bioassays*

Plants for bioassays were grown and tests were performed at 298 K in complete darkness, unless explicitly stated otherwise. Seeds of *Avena sativa* L. cv. Noble (Southern States Farm Cooperative) were soaked in running tap water overnight, sown onto moist vermiculite, covered with a 1 cm layer of vermiculite (clay) and germinated for 5 d, with short exposures to dim green safety light for maintenance. Coleoptiles were harvested under minimal incandescent light and the central leaf was removed. Sections, 9.5 mm in length, were then cut 1.5 mm below the coleoptile tip and temporarily stored in glass-distilled water (pH 5.5). Bioassays were performed on multiwell plates with each well containing ten coleoptile sections in 1 ml of auxin solution (prepared with glass-distilled water). After 24 h of growth, the length of the sections was measured to the nearest 0.5 mm.

Seeds of *Pisum sativum* L. cv. Alaska, inbred line I_3, were obtained courtesy of M. L. Brenner, University

Table 2. *Fractional atomic coordinates and equivalent isotropic displacement parameters (Å^2)*

$$U_{eq} = (1/3)\Sigma_i\Sigma_j U_{ij}a_i^*a_j^*\mathbf{a}_i.\mathbf{a}_j.$$

	x	y	z	U_{eq}
4-F-IAA				
F	0.2411 (1)	0.0038 (2)	0.9763 (3)	0.0672 (8)
O1	0.0858 (2)	0.1096 (2)	0.4472 (3)	0.0465 (9)
O2	0.0785 (1)	−0.0072 (2)	0.6455 (3)	0.0471 (9)
N1	0.2886 (2)	0.2942 (3)	0.7258 (5)	0.057 (1)
C2	0.2088 (3)	0.2797 (3)	0.6967 (5)	0.050 (1)
C3	0.1936 (2)	0.1941 (2)	0.7675 (4)	0.042 (1)
C4	0.2962 (2)	0.0676 (3)	0.9441 (5)	0.050 (1)
C5	0.3747 (3)	0.0487 (4)	1.0108 (7)	0.065 (2)
C6	0.4311 (3)	0.1141 (4)	0.9768 (7)	0.073 (2)
C7	0.4092 (3)	0.1978 (4)	0.8807 (6)	0.064 (2)
C8	0.1125 (2)	0.1536 (3)	0.7613 (5)	0.046 (1)
C9	0.0904 (2)	0.0763 (3)	0.6159 (4)	0.038 (1)
C31	0.2693 (2)	0.1512 (3)	0.8471 (4)	0.041 (1)
C71	0.3283 (2)	0.2158 (3)	0.8162 (5)	0.050 (2)
5-F-IAA				
F	0.5816 (2)	0.7443 (8)	−0.3973 (4)	0.091 (1)
O1	0.9838 (2)	0.7992 (8)	0.0875 (5)	0.071 (1)
O2	0.9183 (2)	0.4317 (9)	0.0051 (5)	0.067 (1)
N1	0.7399 (2)	0.2615 (9)	0.1427 (5)	0.058 (1)
C2	0.8092 (3)	0.397 (1)	0.1994 (7)	0.051 (2)
C3	0.8068 (3)	0.582 (1)	0.0994 (6)	0.040 (2)
C4	0.6939 (3)	0.696 (1)	−0.1665 (7)	0.048 (2)
C5	0.6192 (3)	0.618 (1)	−0.2624 (7)	0.059 (2)
C6	0.5807 (3)	0.412 (1)	−0.2350 (7)	0.065 (2)
C7	0.6163 (3)	0.278 (1)	−0.1015 (7)	0.064 (2)
C8	0.8729 (3)	0.757 (1)	0.1196 (7)	0.049 (2)
C9	0.9255 (3)	0.646 (1)	0.0659 (6)	0.044 (2)
C31	0.7315 (3)	0.561 (1)	−0.0289 (6)	0.040 (1)
C71	0.6923 (3)	0.358 (1)	0.0014 (6)	0.047 (2)
6-F-IAA				
F	0.6457 (2)	0.8955 (4)	0.9806 (1)	0.0330 (7)
O1	0.6043 (2)	1.3028 (4)	0.5185 (1)	0.0235 (7)
O2	0.5978 (2)	0.9195 (4)	0.5755 (1)	0.0220 (7)
N1	0.9071 (3)	0.7498 (6)	0.7590 (2)	0.0196 (8)
C2	0.9005 (3)	0.8768 (6)	0.6906 (2)	0.0173 (9)
C3	0.8040 (3)	1.0729 (6)	0.6910 (2)	0.0171 (9)
C4	0.6465 (3)	1.2224 (6)	0.8004 (2)	0.0184 (9)
C5	0.6141 (3)	1.1622 (7)	0.8727 (2)	0.023 (1)
C6	0.6820 (3)	0.9541 (6)	0.9094 (2)	0.022 (1)
C7	0.7833 (3)	0.8026 (6)	0.8782 (2)	0.021 (1)
C8	0.7615 (3)	1.2454 (7)	0.6261 (2)	0.020 (1)
C9	0.6469 (3)	1.1377 (6)	0.5715 (2)	0.0173 (9)
C31	0.7470 (3)	1.0704 (6)	0.7642 (2)	0.0151 (8)
C71	0.8136 (3)	0.8648 (6)	0.8054 (2)	0.0167 (9)
7-F-IAA				
F	0.4243 (1)	0.6712 (2)	0.4415 (1)	0.0339 (3)
O1	0.1217 (1)	1.2786 (2)	0.0124 (1)	0.0300 (3)
O2	0.1072 (1)	0.9038 (2)	0.0790 (1)	0.0282 (3)
N1	0.4547 (1)	0.7370 (2)	0.2791 (1)	0.0259 (3)
C2	0.4379 (1)	0.8363 (3)	0.2040 (1)	0.0259 (4)
C3	0.3443 (1)	1.0386 (3)	0.1940 (1)	0.0242 (4)
C4	0.2061 (1)	1.2410 (3)	0.2918 (1)	0.0266 (4)
C5	0.1869 (2)	1.2146 (3)	0.3670 (1)	0.0301 (4)
C6	0.2584 (2)	1.0213 (3)	0.4178 (1)	0.0297 (4)
C7	0.3500 (1)	0.8564 (3)	0.3928 (1)	0.0268 (4)
C8	0.2990 (1)	1.2021 (3)	0.1221 (1)	0.0272 (4)
C9	0.1669 (1)	1.1111 (3)	0.0699 (1)	0.0224 (4)
C31	0.2983 (1)	1.0685 (3)	0.2657 (1)	0.0229 (4)
C71	0.3701 (10)	0.8755 (3)	0.3172 (1)	0.0231 (4)

of Minnesota. They were sterilized in 0.05% sodium hypochlorite (*i.e.* 10% of commercial 'Clorox') containing a drop of TWEEN 80 and rinsed under running tap water. The further protocol was essentially the same as for *Avena*, except that the stem sections for the bioassay were cut from the second internode of 10 d old etiolated seedlings.

Table 3. *UV absorption maxima (I–IV; wavelengths in nm) and log ε (in parentheses) for indole-3-acetic acid (IAA) and its ring fluorinated and chlorinated derivatives (for comparison)*

Compounds	(I)	(II)	(III)	(IV)
IAA	219 (4.51)	273 (3.77)	279 (3.78)	288 (3.70)
4-F-IAA	219 (4.583)	266 (3.688)	276 sh (3.627)	285 sh (3.464)
5-F-IAA	222 (4.363)	279 sh (3.800)	286 (3.807)	294 sh (3.721)
6-F-IAA	221 (4.454)	Not visible	283 (3.729)	Not visible
7-F-IAA	217 (4.659)	265 broad (3.741)	280 sh (3.648)	287 (3.559)
4-Cl-IAA	225 (4.551)	276 sh (3.800)	282 (3.830)	291 sh (3.766)
5-Cl-IAA	228 (4.496)	283 sh (3.683)	289 (3.701)	298 sh (3.598)
6-Cl-IAA	228 (4.531)	279 sh (3.753)	285 (3.778)	294 (3.723)
7-Cl-IAA	222 (4.548)	276 sh (3.781)	283 (3.800)	292 sh (3.731)

Table 4. *Retention times in reversed-phase chromatography and lipophilicity parameters (II) for indole-3-acetic acid (IAA) and its ring fluorinated and chlorinated derivatives (for comparison)*

Compound	Retention time (min)	Π
IAA	11.7	0
4-F-IAA	14.5	0.124
5-F-IAA	15.6	0.166
6-F-IAA	16.2	0.186
7-F-IAA	16.0	0.180
4-Cl-IAA	20.3	0.305
5-Cl-IAA	29.5	0.493
6-Cl-IAA	30.2	0.504
7-Cl-IAA	27.1	0.451
K-oxalate (void volume)	3.3	

3. Results

3.1. *Molecular structures in the crystalline state*

Interatomic distances, bond and selected torsion angles for monofluorinated indole-3- acetic acids are listed in Tables 5, 6 and 7. The molecular structures are shown in Fig. 1. Bond distances and angles of the phenyl ring in the monofluorinated indole-3-acetic acids revealed deviations from geometry typical of the aromatic system. A detailed study of substituent effects in benzene on its molecular geometry was given by Domenicano (1992). The electronic properties of indole as an aromatic system are more complex than those of benzene. His observations related to the changes of bond lengths upon substitution cannot be directly correlated with our findings. According to his analysis the two bonds next to the site of substitution should be affected most. The shortening of the C4—C5 bond [1.355 (6) Å] observed in 4-F-IAA is also detected in 4-Cl-IAA [1.368 (6) Å (Nigović *et al.*, 1996)]; this effect is not observed for the C4—C31 bond. The effect of substitution on the endocyclic bond angle at the site of substitution [C—C(X)—C, X = F] observed in this series of compounds revealed the same trend as

Table 5. *Bond lengths (Å) for monofluorinated indole-3-acetic acids*

	4-F-IAA	5-F-IAA	6-F-IAA	7-F-IAA
N1—C2	1.360 (6)	1.376 (8)	1.378 (5)	1.390 (2)
N1—C71	1.373 (6)	1.368 (7)	1.375 (4)	1.369 (2)
C2—C3	1.350 (5)	1.354 (8)	1.358 (4)	1.361 (2)
C3—C31	1.431 (5)	1.431 (8)	1.437 (5)	1.438 (2)
C4—C31	1.386 (6)	1.401 (8)	1.412 (4)	1.405 (2)
C4—C5	1.355 (6)	1.372 (9)	1.374 (5)	1.383 (2)
C5—C6	1.399 (8)	1.382 (9)	1.389 (5)	1.405 (2)
C6—C7	1.369 (8)	1.363 (9)	1.374 (4)	1.368 (2)
C7—C71	1.389 (6)	1.408 (9)	1.379 (5)	1.390 (2)
C31—C71	1.418 (5)	1.391 (8)	1.412 (5)	1.412 (2)
C3—C8	1.501 (5)	1.490 (9)	1.490 (5)	1.495 (2)
C8—C9	1.506 (5)	1.457 (9)	1.505 (5)	1.506 (2)
O1—C9	1.322 (4)	1.301 (7)	1.313 (4)	1.319 (2)
O2—C9	1.206 (5)	1.224 (7)	1.221 (4)	1.222 (2)
F—C4	1.363 (4)			
F—C5		1.358 (7)		
F—C6			1.364 (4)	
F—C7				1.369 (2)

Table 6. *Bond angles (°) for monofluorinated indole-3-acetic acids*

	4-F-IAA	5-F-IAA	6-F-IAA	7-F-IAA
C2—N1—C71	109.3 (4)	108.0 (5)	109.2 (3)	108.6 (1)
N1—C2—C3	110.7 (4)	110.4 (5)	110.0 (9)	110.2 (1)
C2—C3—C8	125.8 (4)	125.1 (5)	125.9 (3)	127.0 (1)
C2—C3—C31	106.4 (4)	106.4 (5)	106.5 (3)	106.7 (1)
C31—C3—C8	127.8 (3)	128.4 (5)	127.5 (3)	126.3 (1)
C3—C31—C4	136.3 (3)	133.8 (5)	134.8 (3)	134.5 (2)
C3—C31—C71	107.0 (3)	107.0 (5)	107.3 (3)	106.4 (1)
C4—C31—C71	116.7 (3)	119.1 (5)	117.9 (3)	119.1 (2)
C31—C4—C5	122.3 (4)	116.4 (6)	119.6 (3)	119.0 (2)
C4—C5—C6	119.3 (5)	124.8 (6)	119.4 (3)	121.5 (2)
C5—C6—C7	121.8 (5)	119.6 (6)	124.0 (3)	119.5 (2)
C6—C7—C71	117.6 (5)	117.1 (6)	115.8 (3)	120.4 (1)
C31—C71—C7	122.3 (4)	122.9 (5)	123.4 (3)	120.5 (1)
N1—C71—C7	131.0 (4)	128.9 (5)	129.7 (3)	131.4 (1)
N1—C71—C31	106.6 (3)	108.2 (5)	107.0 (3)	108.1 (1)
C3—C8—C9	111.3 (3)	114.7 (5)	114.8 (3)	114.8 (1)
C8—C9—O1	112.4 (3)	113.8 (5)	113.1 (3)	112.9 (1)
C8—C9—O2	125.3 (3)	125.6 (6)	124.0 (3)	124.2 (2)
O1—C9—O2	122.3 (3)	120.5 (6)	122.9 (3)	123.0 (1)
C31—C4—F	118.3 (3)			
C5—C4—F	119.4 (4)			
C4—C5—F		117.7 (5)		
C6—C5—F		117.5 (6)		
C5—C6—F			118.2 (3)	
C7—C6—F			117.9 (3)	
C6—C7—F				121.0 (2)
C71—C7—F				118.7 (1)

Table 7. *Selected torsion angles (°) for monofluorinated indole-3-acetic acids*

		4-F-IAA	5-F-IAA	6-F-IAA	7-F-IAA
T_1*	C2—C3—C8—C9	103.3 (4)	87.6 (7)	83.8 (4)	97.2 (2)
	C31—C3—C8—C9	−76.5 (4)	−88.2 (7)	−92.6 (4)	−83.9 (2)
	C3—C8—C9—O1	−62.6 (4)	−178.6 (5)	174.9 (3)	172.1 (1)
T_2	C3—C8—C9—O2	116.8 (4)	1.6 (8)	−5.1 (4)	−8.2 (2)

* Labels used in computational chemistry procedures

described by Domenicano (1992). The electronegative substituent (*X*) enlarges the bond angle C—C(*X*)—C and reduces the adjacent bond angle. In general, such a trend was observed in the series studied (Table 6), although the quantitative relations between these two angles according to Domenicano (1992) cannot be applied. In 4-F-IAA the closing of the C4—C31—C71 angle to 116.7 (3)° is affected by substitution at position 4 of the phenyl ring. The opening of the C4—C5—C6 angle is pronounced for compounds with substituents at position 5 [124.8 (6)°, Table 4; 122.7 (3)° for 5-Cl-IAA and 123.8 (2)° for 5-Br-IAA (Nigović *et al.*, 1996)]. However, a correlation between the angle opening and the size or polarizability of the substituted halogen atoms cannot be found. Contraction of the C6—C7 bond [<1.368 (6) Å>, mean value for the four structures presented in Table 5] is observed in 448 structures ($R < 0.07$) with an indole moiety found in the Cambridge Structural Database (1995; arithmetic mean of 1.376 Å). Closing the C6—C7—C71 angle [<117.3 (6)°> for 4- and 5-F-IAA, and 115.8 (3)° for 6-F-IAA, Table 6] and opening of the C31—C71—C7 angle [<122.9 (4)°>] were observed in the phenyl part of the indole moiety. This distortion of the phenyl part of the indole nucleus was also found in low- and room-temperature diffraction data for IAA (Kojić-Prodić, Puntarec & Nigović, to be published; Chandrasekhar & Raghunathan, 1982). The values from low- and room-temperature experiments are, respectively: C6—C7 1.378 (3), 1.373 (5) Å, and C6—C7—C71 117.4 (2), 117.2 (3)°. It is evident that these deviations from the expected 120° are mainly characteristics of the indole moiety. However, the structure of 7-F-IAA is a single example found with ideal bond angle values of 120°. Deviation of the F atoms from the best least-squares plane of the indole has been observed for 6-F-IAA [0.056 (4) Å] and 7-F-IAA [0.042 (4) Å]. The overall conformation of the molecules is described only by two torsion angles (Table 7). The C2—C3—C8—C9 angle (T_1) defines the relative orientation of a side chain with respect to the indole plane. The orientation of the carboxyl group is given by the C3—C8—C9—O2 angle (T_2). In the crystal structures of the monofluorinated IAA's studied, regardless of the site of substitution, a side chain is close to being perpendicular to the indole plane. The values of the torsion angle C2—C3—C8—C9 range from 83.8 (4) to 103.3 (4)° (Table 7). The conformation about the C8—C9 bond is (+)-synperiplanar (Klyne & Prelog, 1960); the values of the C3—C8—C9—O2 torsion angle are in the range −8.2 (2)–1.6 (8)° (Table 7). However, in the crystal structure of 4-F-IAA the conformation is (+)-anticlinal (Table 7). This very structure is the only example among the structures of indol-3-ylacetic acid conjugates and derivatives with a perpendicular orientation of the carboxyl group to the C3—C8 bond. Although this type of conformation was recognized during the molecular mechanics and dynamics of this series and the *ab inito* calculations of IAA (Ramek, Tomić & Kojić-Prodić, 1995) and 4-Cl- IAA (Ramek, Tomić & Kojić-Prodić, 1996), in this crystal structure it can be related to the formation of the N1—H···F hydrogen bond (to be discussed in the crystal packing section).

3.2. *Crystal packing*

In the crystal structures of monofluorinated IAA's there are two chemically distinct hydrogen bonds acting between: (*a*) carboxylic groups, O1—H···O2, and (*b*) indole and carboxylic groups, N1—H···O1 (Table 8). They produce essentially two different packing arrangements characterized by O—H···O dimers closing an eight-membered ring [$R^2_2(8)$ (Etter, MacDonald & Bernstein, 1990)] and those with both types of hydrogen bonds O—H···O and N—H···O. 5-F-IAA, 6-F-IAA (Fig. 2) and 7-F-IAA (Fig. 3) crystallize in the space group $P2_1/c$ (or its analog $P2_1/a$) and their crystal structures revealed dimers hydrogen bonded *via* carboxylic groups which are also present in the free hormone, IAA (Chandrasekhar & Raghunathan, 1982) and many organic acids (Cambridge Structural Database, 1995), as well as *n*-alkyl-substituted IAA's (Kojić-Prodić, Nigović, Tomić *et al.*, 1991) and achiral amino acid conjugates of IAA (Kojić-Prodić, Nigović, Horvatić *et al.*, 1991). The other type of packing pattern is represented by the crystal structure of 4-F-IAA (Fig. 4) in which N—H···O hydrogen bonds form a 14-membered ring $R^2_2(14)$, whereas both N—H···O and O—H···O generate infinite chains described by graph-set notation as *C*(7) and *C*(9). The hydrogen-bonded dimers of the O—H···O type, present in all centrosymmetric structures of indole-3-acetic acid derivatives, do not occur in this pattern. The lack of dimers might be explained by the anticlinal conformation about the C8—C9 bond. In all other structures studied (±)-synperiplanar conformation occurs, which favors hydrogen-bonded dimers. Instead, O—H···O hydrogen bonds link the molecules into an infinite chain along **c**. The indole N—H is involved in bifurcated hydrogen bonds to a hydroxyl group and a F atom (Table 8), which complete the crystal packing. Halogen atoms can

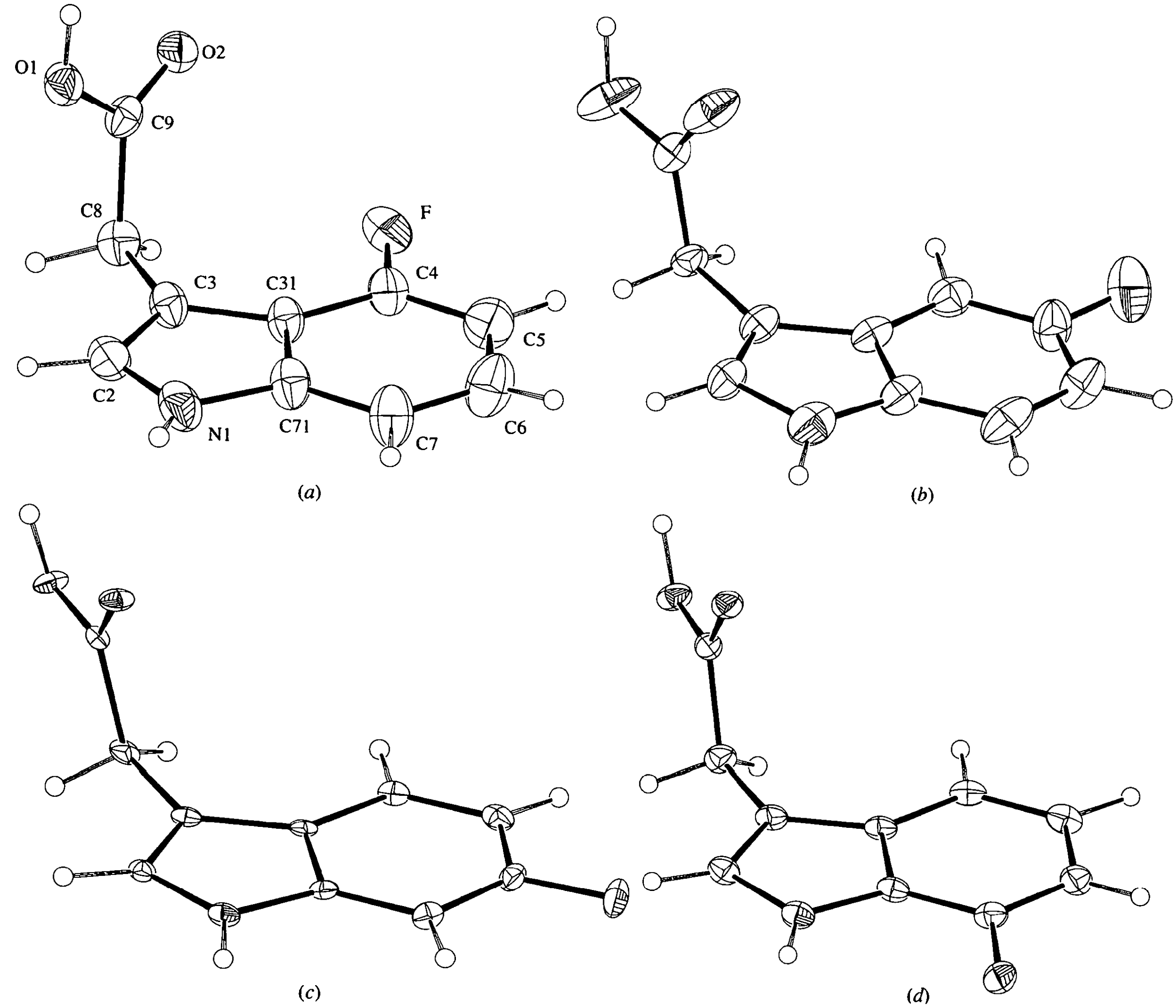

Fig. 1. Molecular structures (*ORTEP*II; Johnson, 1976) of monofluorinated indol-3-ylacetic acids: (*a*) 4-F-IAA, (*b*) 5-F-IAA, (*c*) 6-F-IAA and (*d*) 7-F-IAA. Atom numbering is shown for 4-F-IAA. The thermal ellipsoids are scaled at the 30% probability level.

Table 8. *Hydrogen bonds, C—H···X (X = O, F) and N—H···C (phenyl) contacts in the structures of monofluorinated indole-3-acetic acids*

Compound		$D\cdots A$ (Å)	D—H (Å)	H···A (Å)	D—H···A (°)
4-F-IAA	O1—H···O2^{i}	2.634 (3)	0.84 (4)	1.84 (4)	157 (4)
	N1—H···O1^{ii}	3.082 (5)	0.83 (5)	2.36 (5)	146 (5)
	N1—H···F^{iii}	3.258 (5)	0.83 (5)	2.61 (5)	136 (5)
5-F-IAA	O1—H···O2^{iv}	2.717 (6)	0.98 (3)	1.75 (4)	168 (3)
	C2—H···O2^{v}	3.256 (8)	0.97 (3)	2.40 (3)	146 (2)
	N1—H···C4^{v}	3.367 (8)	0.90 (3)	2.50 (3)	164
	N1—H···C5^{v}	3.470	0.90 (3)	2.70 (4)	144
6-F-IAA	O1—H···O2^{vi}	2.696 (4)	0.95 (5)	1.76 (5)	171 (4)
	C2—H···O2^{vii}	3.228 (4)	1.00 (4)	2.26 (4)	163 (3)
	C7—H···F^{viii}	3.306 (4)	1.07 (3)	2.33 (3)	151 (2)
	N1—H···C4^{vii}	3.361 (4)	0.98 (4)	2.413	164
	N1—H···C5^{vii}	3.442 (5)	0.98 (4)	2.515	159
7-F-IAA	O1—H···O2^{ix}	2.657 (2)	0.98 (3)	1.67 (3)	177 (3)
	C2—H···O2^{vii}	3.267 (2)	0.96 (2)	2.31 (2)	177 (1)
	N1—H···C4^{vii}	3.432 (2)	0.89 (2)	2.65	148
	N1—H···C5^{vii}	3.366 (2)	0.89 (2)	2.48	173

Symmetry codes: (i) $x, -y, z-\frac{1}{2}$; (ii) $\frac{1}{2}-x, \frac{1}{2}-y, 1-z$; (iii) $\frac{1}{2}-x, \frac{1}{2}+y, \frac{3}{2}-z$; (iv) $2-x, 1-y, -z$; (v) $x, \frac{1}{2}-y, z+\frac{1}{2}$; (vi) $1-x, 2-y, 1-z$; (vii) $x+\frac{1}{2}, \frac{3}{2}-y, z$; (viii) $\frac{3}{2}-x, y-\frac{1}{2}, 2-z$; (ix) $-x, 2-y, -z$.

be hydrogen-bond acceptors (Jeffrey & Saenger, 1991; Desiraju & Parthasarathy, 1989). The acceptor function of the F atom can be expected from its electronegativity, but is poorly documented. By inspection of the Cambridge Structural Database (1995) using the coded fragment N—H···F—C, 77 structures (with $R \leq 0.06$) with the contacts N···F ranging from 2.850 to 3.30 Å were selected. The values of the N—H···F angle were frequently in the range 90–120°, suggesting a three-centered (bifurcated) hydrogen bond. The geometry of C7—F···H—N interactions observed in the structures discussed is in agreement with those reported for some fluorine-containing organic compounds (Shimoni & Glusker, 1994).

In addition to the classical type of hydrogen bonds detected in the structures studied, weak C—H···O [4.19–8.37 kJ mol^{-1} (Desiraju, 1991)] and N—H···C(phenyl) [8.37–16.75 kJ mol^{-1} (Perutz, 1993)] interactions were observed; they are present in the crystal structures lacking N—H···O hydrogen bonds. In the crystal structures of 5-F-IAA, 6-F-IAA and 7-F-IAA intermolecular C—H···O interactions, between the C2sp^2 atom of the pyrrole ring and the C=O part of the carboxylic group, are present. The geometry observed (Table 8) is in agreement with the criteria described by Taylor & Kennard (1982), Berkovich-Yellin & Leiserowitz (1984) and Desiraju (1991). The occurrence of C—H···O interactions in auxin derivatives and analogs was discussed recently by Kojić-Prodić, Kroon & Puntarec (1994). The N—H···phenyl interactions contribute to the packing of 5-F-IAA, 6-F-IAA and 7-FIAA; N1—H points to the C4—C5 bond (Table 8). They were detected by the crystal packing lacking N—H···O hydrogen bonds. The N—H···C(phenyl) interaction might be important for substrate binding to the auxin-binding protein (or a receptor). Both, indole and non-indole auxins

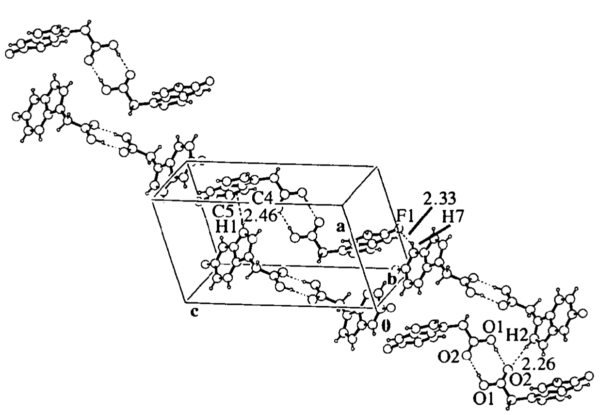

Fig. 2. Molecular packing of 6-F-IAA with O—H···O and N—H···O hydrogen bonds and C—H···F contacts.

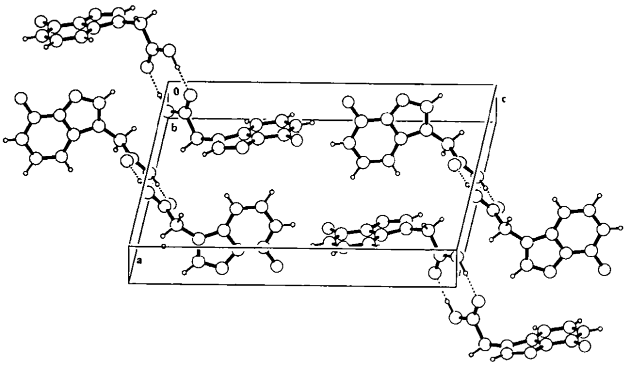

Fig. 3. Molecular packing of 7-F-IAA with O—H···O hydrogen bonds.

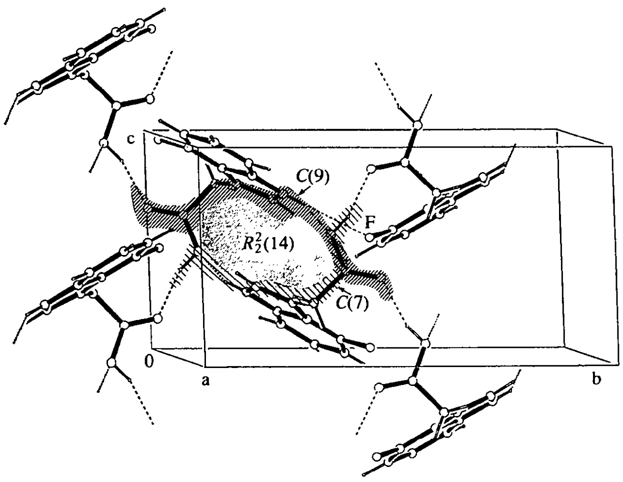

Fig. 4. Molecular packing of 4-F-IAA with O—H···O and N—H···O hydrogen bonds, which can be described as follows: $R_2^2(14)$ motif is generated by N1—H···O1, whereas $C(7)$ and $C(9)$ are produced by N1—H···O1 and O1—H···O2 interactions. The crystal packing is completed by an N1—H···F interaction with H1 bifurcated between O1 and F.

Table 9. *Conformational analysis of monofluorinated IAA about the C3—C8 and C8—C9 bonds*

Calculations were perfomed by *DISCOVER* [Biosym Technologies, 1994 (CVFF)]. Torsion angles (°)* refer to: C2—C3—C8—C9, first entry; C3—C8—C9—O2, second entry

	4-F-IAA		5-F-IAA		6-F-IAA		7-F-IAA	
X-ray analysis	103.3	116.8	87.6	1.6	83.8	−5.1	97.2	−8.2
Molecular mechanics								
Input atomic coordinates: X-ray data								
(*a*) Molecule optimized *in vacuo* without constraint	90	99	94	95	94	−95	94	−95
(*b*) Molecule optimized *in vacuo* with tethering† to the conformation found in the crystal	101.8	115.0	87.3	−0.3	86.1	−10.7	95.3	−8.3
ΔE [between (*a*) and (*b*): $E_b - E_a$] (kJ mol^{-1})	2.09		10.05		10.47		10.05	

* The molecules studied are achiral and the sign of the torsion angles is relevant in the comparison of relative orientations of the carboxylic group and indole moiety only. † A penalty function is used which keeps the atoms close to their initial positions.

contain an aromatic nucleus which can interact with the auxin-binding protein active site (Edgerton, Tropsha & Jones, 1994). The first evidence of an acceptor function of the aromatic ring in hydrogen bonding was given by Klemperer, Cronyn, Maki & Pimentel (1954). The energetical and geometrical criteria were discussed by Levitt & Perutz (1988). The stabilizing role in the structure of α-helices of proteins has been recognized (Perutz, 1993; Hunter, 1993). A somewhat different opinion was expressed by Mitchell, Nandi, McDonald, Thornton & Price, 1994. These authors detected N—H···C hydrogen bonds, but found them to be rare and not stable enough to represent a significant contribution to protein stability. Evidence for N—H···C hydrogen bonding in crystalline alkynes, alkenes and aromatics (Viswamitra, Radhakrishnan, Bandekar & Desiraju, 1993) contribute to the knowledge of this unusual interaction. To obtain consistent knowledge on this topic more examples should be studied.

3.3. *Molecular mechanics and molecular dynamics*

Kaethner (1977) related the biological activity of the auxins to the flexibility of the side chain. The conformational search for monofluorinated IAA's was performed by *DISCOVER* (Biosym Technologies, 1994) with the CVFF force field (Dauber-Osguthorpe *et al.*, 1988). Complete energy optimization of the crystallographically determined structures was performed *in vacuo* for each molecule: (*a*) without any constraint and (*b*) using a penalty function which kept the atoms close to their initial positions. The results are summarized in Table 9. For all compounds the conformer with the anticlinal conformation (+ or −) about the C3—C8 bond was determined as the most stable; during the optimization the conformation about the C3—C8 bond remained anticlinal (as in the crystal). This was also the case for the conformation about the C8—C9 bond of 4-F-IAA; the synperiplanar orientation about the C8—C9 bond determined in the crystals of the other F-IAA's changed during the optimization to anticlinal (Table 9). The conformational search was accomplished by rotations about the pair of bonds C3—C8 and C8—C9, in steps of 15° (CVFF). The results obtained are similar to those obtained for earlier analyzed monohalogenated IAA's (Nigović *et al.*, 1996). The minima located in two-dimensional space are: $T_1 \simeq 90 \pm 30$, $T_2 \simeq 90 \pm 30$ and $T_1 \simeq 90 \pm 30$, $T_2 \simeq -90 \pm 30°$ (molecule is achiral and the conformations $T_1 = -90 \pm 30$, $T_2 = -90 \pm 30$ and $T_1 = -90 \pm 30$, $T_2 = 90 \pm 30°$ are identical mirror images of each other). Transitions between these regions are frequent during simulations *in vacuo* (250 ps of simulation was performed at increasing temperatures 300–450 K) and occur mostly through the saddle points at $T_1 \sim 90$, $T_2 \sim 0$ and $T_1 \sim 0$, $T_2 \sim 90°$. To simulate natural conditions and to evaluate the influence of solvent on the conformational behavior of the compounds, molecular dynamics simulations in water (Fig. 5) were performed using periodic boundary conditions. Each compound was simulated for *ca* 250 ps. The conditions during the simulations were as specified earlier (Nigović *et al.*, 1996). During the simulations

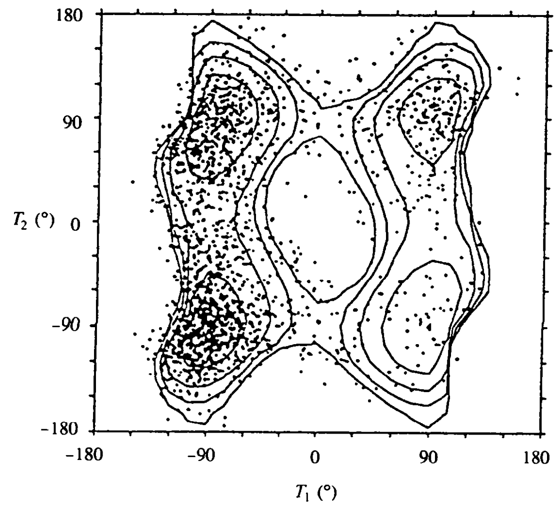

Fig. 5. Molecular dynamics simulation for 4-F-IAA in water at elevated temperatures (300–450 K) over 250 ps. The values of torsional angles T_1 and T_2 (°), obtained during the simulations, are superimposed on the contour graph (the energy intervals are 8.37 kJ mol^{-1}).

water transitions about the C3—C8 bond were rare at temperatures below 400 K. As noticed earlier, the region about the saddle point $T_1 \sim 90$ (±30°), $T_2 \sim 0$ (±30°) is more populated in water than *in vacuo*.

For fluorinated IAA's *ab initio* results are not available, but on the basis of the results obtained for indol-3-ylacetic acid (Ramek, Tomić & Kojić-Prodić, 1995) and 4-Cl-IAA (Ramek, Tomić, Kojić-Prodić, 1996), and of the close analogy of the molecular mechanics results obtained for all halogenated compounds, the planar conformation ($T_1 \simeq 0$, $T_2 \simeq 0°$) might also be possible.

3.4. *Auxin activity*

In bioassays based on the elongation of stem (coleoptile) sections the ring-fluorinated IAA's were equally or more effective auxins than the unsubstituted parent compound. The results of an *Avena* coleoptile straight-growth test are presented in Fig. 6. The dose–response curves were approximated by polynomials fitted to the experimental data. The response to IAA, 5-F-IAA and 7-F-IAA (Fig. 6*a*) could be presented by the same regression curve, without a major loss of accuracy; coleoptile sections supplied with 6-F-IAA grew slightly but consistently longer, throughout the range of concentrations examined; both dose–response curves (Fig. 6*a*) peaked at the optimal concentration of 9×10^{-3} mmol l^{-1}. 4-F-IAA was considerably more active in *Avena*. The dose–response curve was thus examined for a wider range of concentrations, in a separate experiment (Fig. 6*b*). A series of dilutions of IAA was tested with the same coleoptile sections to account for batch-to-batch differences in auxin sensitivity. Throughout its

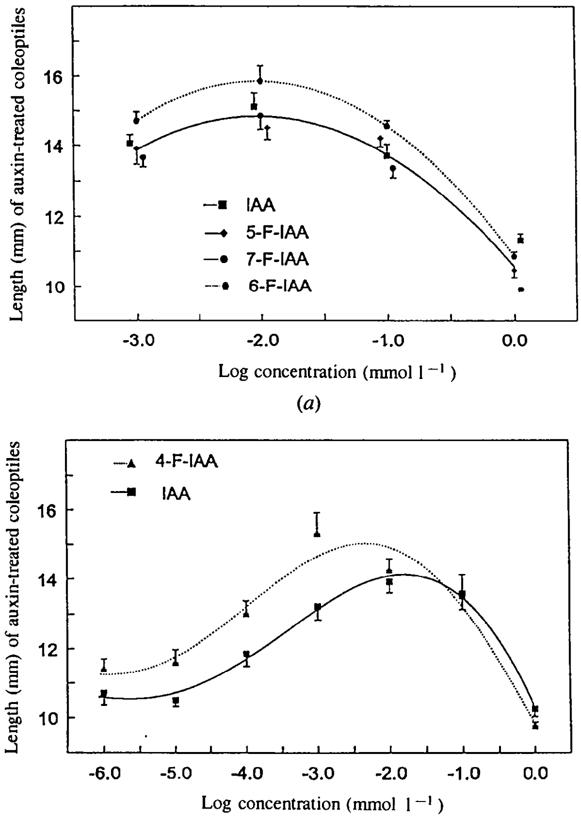

Fig. 6. Growth-promoting properties, in the *Avena* coleoptile straight-growth test, of IAA (squares), 4-F-IAA (triangles), 5-F-IAA (diamonds), 6-F-IAA (hexagons) and 7-F-IAA (filled circles). (*a*) and (*b*) represent different experiments. The dose–response curves shown are based on the following regression equations [x = log concentration (mmol l^{-1}); y = length (mm)]. (*a*) 6-F-IAA: $y = 10.85 - 4.92x - 1.21x^2$ ($n = 4$, $r = 0.999$, $s_{y.x} = 0.011$); other compounds: $y = 10.56 - 4.21x - 1.04x^2$ ($n = 12$, $r = 0.975$, $s_{y.x} = 0.425$). (*b*) 4-F-IAA: $y = 9.808 - 3.682x + 0.137x^2 + 0.537x^3 + 0.105x^4 + 0.00582x^5$ ($n = 8$, $r = 0.978$, $s_{y.x} = 0.722$); IAA: $y = 10.27 - 4.683x - 1.558x^2 - 0.0293x^3 + 0.0355x^4 + 0.00276x^5$ ($n = 8$, $r = 0.996$, $s_{y.x} = 0.257$). The response (not shown) at an auxin concentration of 10^{-7} mmol l^{-1} was essentially the same as for 10^{-6} mmol l^{-1}.

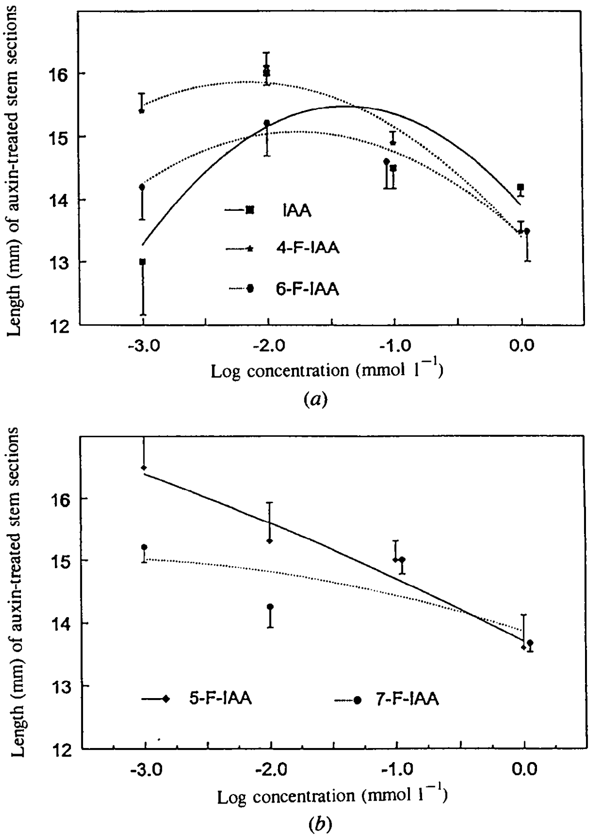

Fig. 7. Growth-promoting properties, in the *Pisum sativum* straight-growth test, of IAA (squares, solid line), 4-F-IAA (stars, dotted line), 5-F-IAA (diamonds, solid line), 6-F-IAA (hexagons, dotted line) and 7-F-IAA (filled circles, dotted line). (*a*) and (*b*) represent results from the same experiment. The dose–response curves shown are based on the following regression equations (x and y defined as in Fig. 6). IAA: $y = 13.92 - 2.27x - 0.83x^2$ ($n = 4$, $r = 0.803$, $s_{y.x} = 1.275$); 4-F-IAA: $y = 13.42 - 2.27x - 0.53x^2$ ($n = 4$, $r = 0.980$, $s_{y.x} = 0.380$); 5-F-IAA: $y = 13.70 - 1.05x - 0.05x^2$ ($n = 4$, $r = 0.976$, $s_{y.x} = 0.447$); 6-F-IAA: $y = 13.45 - 1.85x - 0.53x^2$ ($n = 4$, $r = 0.980$, $s_{y.x} = 0.246$); 7-F-IAA: $y = 13.86 - 0.67x - 0.095x^2$ ($n = 4$, $r = 0.721$, $s_{y.x} = 0.845$).

ascending part, the dose–response curve for 4-F-IAA was considerably above that for IAA and the optimal concentration of the fluorinated analog was significantly smaller (ten times, as determined from the original measurements; *ca* five times according to the regression curves).

The results for the pea-stem straight-growth test (Figs. 7*a* and *b*) were more variable and should be interpreted in a more qualitative fashion. The optimal concentrations for IAA, 4-F-IAA and 6-F-IAA were around 10^{-2} mmol l^{-1}; the lower value ($\sim 10^{-3}$ mmol l^{-1}) deduced for 7-F-IAA may well be inaccurate, due to the unreasonably weak response at 10^{-2} mmol l^{-1}. Only 5-F-IAA appears to be considerably more active than the other compounds tested. Its auxin activity in *Pisum sativum* stems has already been reported to be higher than in coleoptiles of *Avena* or *Triticum* (Hoffmann, Fox & Bullock, 1952; Porter & Thimann, 1965; Böttger, Engvild & Soll, 1978; Katekar & Geissler, 1983; Zažimalova & Kutaček, 1985).

4. Conclusions

The plant growth-promoting properties of ring-substituted IAA's are far from being fully understood. Here we show, surprisingly for the first time, that fluorination at any of the four positions in the phenyl ring yields auxins of high activity in stem(coleoptile)-elongation assays. Moreover, 4-F-IAA is one of the most effective auxins in *Avena*, while 5-F-IAA appears to be more stimulatory in *Pisum sativum*. Attempts have been made to link biological activity to lipid solubility, to the electron distribution in the indole nucleus and to the stereochemistry of the CH_2COOH moiety. However, these properties are not substantially affected by fluorination. The increments in lipophilicity (Π; Table 4) are position dependent and two to three times smaller than for the corresponding chloroindole-3-acetic acids (for reference values measured by partition in *n*-octanol/water, *cf.* Katekar & Geissler, 1982). The electron (UV) spectra show small differences in the relative intensities of the three long-wavelength absorbance maxima (Table 3). While the tops of these very broad peaks are difficult to assign with accuracy, the shifts with respect to the spectrum of unsubstituted IAA appear to be, at least in most cases, smaller than for the corresponding chloro analogs, the only ring-halogenated IAA's tested so far systematically. The UV spectrum of unsubstituted IAA was analyzed in detail by Tomas-Vert *et al.* (1991). In the UV spectra of halogenated IAA's an autochrome effect (changes in wavelength and intensity) was expected which normally occurs when Cl or F are attached to a chromophore (phenyl). However, this effect appears to be too small to allow quantitative analysis of transfers from the bonding to the antibonding state of chromophores introduced by halogenation of the phenyl moiety. In general, small differences can be detected between Cl-IAA's and F-IAA's; in 4-F-IAA lines are shifted to shorter wavelength compared with 4-Cl-IAA. In the spectra of Cl-IAA's the effect of the site of substitution is not pronounced. These spectroscopic findings are generally in agreement with observations on molecular geometry of halogenated IAA's; the molecular geometry of the phenyl ring is affected by halogenation at position 4 only. These experimental data suggest that the aromatic nucleus is well-balanced electronically. The rotational freedom of the CH_2COOH chain and its preferred conformations in solution are not affected by fluorination in the phenyl nucleus.

Based on the physical properties of ring-fluorinated IAA's, it is thus not surprising that their auxin properties are so similar to those of the unsubstituted parent compound. Species-specific properties of auxin receptors may explain the outstanding activity of 4-F-IAA in *Avena* coleoptiles and 5-F-IAA in *Pisum sativum*; however, differences in metabolic stability may be more likely. There are relatively few reports on catabolic pathways involving attack on the phenyl part of the IAA molecule (*e.g.* Bandurski, Cohen, Slovin & Reinecke, 1995; Marumo, 1986), but the likely products, ring-hydroxylated indoles, are hydrophilic and autooxidizable and could be overlooked in some standard screening procedures.

Half-optimal concentrations derived from dose–response curves have been used as estimates for the dissociation constants (K_d) of the auxin–receptor complexes which trigger the growth effect (Libbenga, Maan, van den Linde & Mennes, 1986). The respective values obtained from the regression curves in Figs. 6 and 7 are 8×10^{-8} to 4×10^{-7} mol l^{-1} for *Avena* and (as far as estimates are possible) 2×10^{-7} to 2×10^{-6} mol l^{-1} for *Pisum sativum*. These numbers are indeed of the same order of magnitude as the reported dissociation constants for IAA binding to a crude membrane fraction from *Avena* coleoptiles [2×10^{-7} mol l^{-1} for 'high-affinity' binding (Bhattacharrya & Biswas, 1982)] and plasma membranes from pea epicotyls [1×10^{-6} mol l^{-1} (Döllstädt, Hirschberg, Winkler & Hübner, 1976)]. When IAA and its fluorinated analogs attach to the respective binding sites, this would, at 298 K, set free an energy (calculated as $\Delta G = RT\ln K_d$), where $\Delta G \simeq -29.3$ to -41.9 kJ mol^{-1}, which could then be used for rotation of the CH_2COOH group (Kubinyi, 1993). Unfortunately, it is not known which fraction of the binding energy is consumed for conformational changes in the receptor protein itself. It appears unwise to base structure–activity correlations on fixed conformations of the auxin molecule, as advocated by nearly all previous workers in this field.

This work was supported in part by the Ministry of Science and Technology, Republic of Croatia grants numbers 1-07-179 and 1-08-195. The authors thank

Dr M. Žinić, Rudjer Bošković Institute, Zagreb, for constructive discussion.

References

B. A. Frenz & Associates, Inc. (1982). *SDP Structure Determination Package*. College Station, Texas, USA.

Bandurski, R. S., Cohen, J. D., Slovin, J. & Reinecke, D. M. (1995). *Plant Hormones: Physiology, Biochemistry and Molecular Biology*, edited by P. Davies, pp. 38–65. Dordrecht: Kluwer Academic Publishers.

Bergmann, E. D. & Pelchowicz, Z. (1959). *J. Chem. Soc.* pp. 1913–1914.

Berkovitch-Yellin, Z. & Leiserowitz, L. (1984). *Acta Cryst.* B**40**, 159–165.

Bhattacharrya, K. & Biswas, B. B. (1982). *Phytochemistry*, **21**, 1207–1211.

Biosym Technologies (1994). *DISCOVER*. Version 2.9.5. Biosym Technologies, 1065 Barnes Canyon Rd, San Diego, CA 92121, USA.

Bondi, A. (1964). *J. Phys. Chem.* **68**, 441–451.

Böttger, M., Engvild, K. C. & Soll, H. (1978). *Planta*, **140**, 89–92.

Cambridge Structural Database (1995). Version 5.09. Cambridge Crystallographic Data Centre, 12 Union Road, Cambridge, England.

Chandrasekhar, K. & Raghunathan, S. (1982). *Acta Cryst.* B**38**, 2534–2535.

Dauber-Osguthorpe, P., Roberts, V. A., Osguthorpe, D. J., Wolff, J., Genest, M. & Hagler, A. T. (1988). *Proteins Struct. Funct. Genet.* **4**, 31–47.

Desiraju, G. R. (1991). *Acc. Chem. Res.* **24**, 290–296.

Desiraju, G. R. & Parthasarathy, R. (1989). *J. Am. Chem. Soc.* **111**, 8725–8726.

Döllstädt, R., Hirschberg, K., Winkler, E. & Hübner, G. (1976). *Planta*, **130**, 105–111.

Domenicano, A. (1992). *Accurate Molecular Structures*, edited by A. Domenicano & I. Hargittai, pp. 436–468. Oxford University Press.

Edgerton, M. D., Tropsha, A. & Jones, A. M. (1994). *Phytochemistry*, **35**, 1111–1123.

Engvild, K. C. (1978). *Physiol. Plant.* **44**, 345–346.

Etter, M. C., MacDonald, C. & Bernstein, J. (1990). *Acta Cryst.* B**46**, 256–262.

Filler, R. (1993). *Organofluorine Compounds in Medicinal Chemistry and Biomedical Applications*, edited by R. Filler, Y. Kobayashi & L. M. Yagupolskii, pp. 1–22. Amsterdam: Elsevier.

Fujita, T., Iwasa, J. & Hansch, C. (1964). *J. Am. Chem. Soc.* **86**, 5175–5180.

Hoffmann, O. L., Fox, S. W. & Bullock, M. W. (1952). *J. Biol. Chem.* **196**, 437–441.

Hunter, C. A. (1993). *Phil. Trans. R. Soc. A*, **345**, 77–85.

Jeffrey, G. A. & Saenger, W. (1991). *Hydrogen Bonding in Biological Structures*. Berlin: Springer Verlag.

Johnson, C. K. (1976). *ORTEP*II. Report ORNL-5138. Oak Ridge National Laboratory, Tennessee, USA.

Kaethner, T. M. (1977). *Nature* (*London*), **267**, 19–23.

Katayama, M., Kato, K., Kimoto, H. & Fuji, S. (1995). *Experientia*, **51**, 721–724.

Katekar, G. F. & Geissler, A. E. (1982). *Phytochemistry*, **21**, 257–260.

Katekar, G. F. & Geissler, A. E. (1983). *Phytochemistry*, **22**, 27–31.

Klemperer, W., Cronyn, M. W., Maki, A. M. & Pimentel, G. C. (1954). *J. Am. Chem.* Soc. **76**, 5846–5848.

Klyne, W. & Prelog, V. (1960). *Experientia*, **16**, 521–568.

Kojić-Prodić, B., Kroon, J. & Puntarec, V. (1994). *J. Mol. Struct.* **322**, 43–69.

Kojić-Prodić, B., Nigović, B., Horvatić, D., Ružić-Toroš, Ž., Magnus, V., Duax, W. L., Stezowski, J. J. & Bresciani-Pahor, N. (1991). *Acta Cryst.* B**47**, 107–115.

Kojić-Prodić, B., Nigović, B., Tomić, S., Ilić, N., Magnus, V., Konjević, R., Giba, Z. & Duax, W. L. (1991). *Acta Cryst.* B**47**, 1010–1019.

Kojić-Prodić, B., Puntarec, V. & Nigović, B. *Low Temperature Data for IAA*. To be published.

Krstulović, A. M. & Brown, P. R. (1982). *Reversed-Phase High Performance Liquid Chromatography*. New York: Wiley & Sons.

Kubinyi, H. (1993). Editor. *3D QSAR in Drug Design Theory, Methods and Applications*. Leiden: ESCOM.

Leo, A., Hansch, C. & Elkins, D. (1971). *Chem. Rev.* **71**, 525–616.

Levitt, M. & Perutz, M. F. (1988). *J. Mol. Biol.* **201**, 751–754.

Libbenga, K. R., Maan, A. C., van den Linde, P. C. G. & Mennes, A. M. (1986). *Hormones, Receptors and Cellular Interactions in Plants*, edited by C. M. Chadwick & D. R. Garrod, pp. 1–68. Cambridge University Press.

Marumo, S. (1986). *Chemistry of Plant Hormones*, edited by N. Takahashi, pp. 9–56. Boca Raton, Florida: CRC Press.

Mitchell, J. B. O., Nandi, C. L., McDonald, I. K., Thornton, J. M. & Price, S. L. (1994). *J. Mol. Biol.* **239**, 315–331.

Nigović, B., Kojić-Prodić, B., Antolić, S., Tomić, S., Puntarec, V. & Cohen, J. D. (1996). *Acta Cryst.* B**52**, 332–343.

Perutz, M. F. (1993). *Phil. Trans. R. Soc. London A*, **345**, 105–112.

Porter, W. L. & Thimann, K. V. (1965). *Phytochemistry*, **4**, 229–243.

Ramek, M., Tomić, S. & Kojić-Prodić, B. (1995). *Int. J. Quantum Chem. Quantum Biol. Symp.* **22**, 75–81.

Ramek, M., Tomić, S. & Kojić-Prodić, B. (1996). *Int. J. Quantum Chem. Quantum Biol. Symp.* In the press.

Reinecke, D., Ozga, J. & Magnus, V. (1995). *Phytochemistry*, **40**, 1361–1366.

Sheldrick, G. M. (1976). *SHELX76. Program for Crystal Structure Determination*. University of Cambridge.

Sheldrick, G. M. (1985). *Crystallographic Computing 3*, edited by G. M. Sheldrick, C. Krüger & R. Goddard, pp. 175–189. Oxford University Press.

Shimoni, L. & Glusker, J. P. (1994). *Struct. Chem.* **5**, 383–397.

Somei, M., Kizu, K., Kunimoto, M. & Yamada, F. (1985). *Chem. Pharm. Bull.* (*Tokyo*), **33**, 3696–3708.

Spek, A. L. (1982). *The EUCLID Package. Computation Crystallography*, edited by D. Sayre, p. 528. Oxford: Clarendon Press.

Taylor, R. & Kennard, O. (1982). *J. Am. Chem. Soc.* **104**, 5063–5070.

Tomas-Vert, F., Ponce, C. A., Estrada, M. R., Silber, J., Singh, J. & Anunciatta, J. (1991). *J. Mol. Struct.* **246**, 203–215.

Viswamitra, M. A., Radhakrishnan, R., Bandekar, J. & Desiraju, G. R. (1993). *J. Am. Chem. Soc.* **115**, 4868–4869.

Zažimalova, E. & Kutaček, M. (1985). *Biol. Plant.* (*Praha*), **27**, 114–118.